

**Measuring cosmological bulk flows via the kinematic  
Sunyaev-Zeldovich effect in the upcoming cosmic microwave  
background maps.**

A. Kashlinsky

Raytheon ITSS

Code 685, Goddard Space Flight Center, Greenbelt, MD 20771

e-mail: kashlinsky@stars.gsfc.nasa.gov

F. Atrio-Barandela

Física Teórica. Facultad de Ciencias.

Universidad de Salamanca, 37008 Spain.

e-mail: atrio@orion.usal.es

Received \_\_\_\_\_; accepted \_\_\_\_\_

## ABSTRACT

We propose a new method to measure the possible large-scale bulk flows in the Universe from the cosmic microwave background (CMB) maps from the upcoming missions, MAP and Planck. This can be done by studying the statistical properties of the CMB temperature field at many X-ray cluster positions. At each cluster position, the CMB temperature fluctuation will be a combination of the Sunyaev-Zeldovich (SZ) kinematic and thermal components, the cosmological fluctuations and the instrument noise term. When averaged over many such clusters the last three will integrate down, whereas the first one will be dominated by a possible bulk flow component. In particular, we propose to use all-sky X-ray cluster catalogs that should (or could) be available soon from X-ray satellites, and then to evaluate the dipole component of the CMB field at the cluster positions. We show that for the MAP and Planck mission parameters the dominant contributions to the dipole will be from the terms due to the SZ kinematic effect produced by the bulk flow (the signal we seek) and the instrument noise (the noise in our signal). Computing then the expected signal-to-noise ratio for such measurement, we get that at the 95% confidence level the bulk flows on scales  $\geq 100h^{-1}\text{Mpc}$  can be probed down to the amplitude of  $< 200 \text{ km/sec}$  with the MAP data and down to only  $\simeq 30 \text{ km/sec}$  with the Planck mission.

*Subject headings:* Cosmology: Cosmic Microwave Background. Large Scale Structure. Galaxies: Clusters.

## 1. Introduction.

Peculiar motions trace the overall mass distribution and it is important to determine the coherence scale and amplitude of bulk flows. Current measurements range from bulk flows as high as 700 km/sec on scale of  $\sim 150h^{-1}\text{Mpc}$  (Lauer & Postman 1994) to finding little peculiar motion on scales beyond  $\sim 70h^{-1}\text{Mpc}$  (see Willick 2000 for review). It is thus important to find alternative ways to test for such bulk flows. One alternative way to measure peculiar flows is via the kinematic Sunyaev Zeldovich (SZ) effect produced on the cosmic microwave background (CMB) photons from the hot X-ray emitting gas in clusters of galaxies (Zeldovich & Sunyaev 1969). Such program is already being undertaken in the SuZIE project which plans to measure motion of 40 clusters at  $z=0.1-0.3$  and determine the peculiar velocity of each cluster to a precision of 700 km/sec.

In this *letter* we propose to use CMB data from the MAP and Planck missions to measure the bulk flows in a quick, cheap and efficient way. X-ray cluster catalogs to be available shortly based on ROSAT, ASCA and XMM measurements, will provide locations of the SZ sources on the CMB sky and a reasonable estimate of the cluster electron density distribution and temperature. If there are significant bulk motions they will leave an imprint via the cumulative kinematic SZ effect and can be uncovered by cross-correlating the temperature field at the cluster positions in the MAP and Planck CMB maps. Such bulk motions would produce a significant dipole component in the temperature field evaluated at the cluster locations. By averaging temperature fields at enough cluster positions, the thermal SZ and other noise components will integrate down enough to reveal possible bulk motions out to  $\sim 300-400$  km/s on scales  $\geq 50-100h^{-1}\text{Mpc}$ .

## 2. Dipole of the cumulative SZ kinematic effect.

Consider the CMB field at a beam centered on one isothermal X-ray emitting cluster at the angular position  $\vec{y}$ . If the cluster is moving with the line-of-sight velocity  $v_r$  with respect to the CMB rest frame, the SZ CMB fluctuation at frequency  $\nu$  at this position will be  $\delta_\nu(\vec{y}) = \delta_{th}(\vec{y})G(\nu) + \delta_{kin}(\vec{y})H(\nu)$ , with  $\delta_{th} = \tau T_{\text{virial}}/T_{e,ann}$  and  $\delta_{kin} = \tau v_r/c$  (e.g. Phillips 1995). Here  $\tau$  is the projected optical depth due to Compton scattering,  $T_{\text{virial}}$  is the cluster virial temperature and  $k_B T_{e,ann} = 0.5$  MeV. (For expressions for the spectral dependence of the two SZ components,

$G(\nu), H(\nu)$  see e.g. Birkinshaw (1999).) Normally the thermal term dominates for individual clusters, but if averaged over many clusters moving at a significant bulk flow with respect to the CMB rest-frame, the former will integrate down  $\propto 1/N_{\text{cluster}}$ , while the kinematic term will reflect coherent motions with amplitude  $V_{\text{bulk}}$ .

In order to minimize the contribution from other sources, we will start with CMB maps from which the cosmological dipole component was subtracted down to  $\sigma_d$ . This uncertainty is already  $\sigma_d = 7\mu\text{K}$  (Fixsen et al. 1996) and should be significantly smaller in MAP observations. The MAP radiometers produce a raw temperature measurement that is the difference between two points on the sky  $\sim 140^\circ$  apart which introduces an error on the dipole determination, due to correlated noise, of the order of  $0.1\mu\text{K}$ ; the dominant uncertainty in the dipole will be due to confusion from the galactic foreground (G. Hinshaw, private communication). After the cosmological CMB dipole subtraction the CMB fluctuation in band  $\nu$  at position  $\vec{y}$  centered on a known X-ray cluster will be  $\delta_\nu(\vec{y}) = \delta_{th}(\vec{y})G(\nu) + [\delta_{kin}(\vec{y}) + \delta_{\text{CMB}}(\vec{y})]H(\nu) + r(\nu)$ . Here  $r(\nu)$  is the instrument noise at frequency  $\nu$  and  $\delta_{\text{CMB}}(\vec{y})$  is the cosmological CMB component whose dipole is now  $\sigma_d^2$ . Consider the dipole component of  $\delta_\nu(\vec{y})$  with the dipole amplitude  $C_1$  normalized so that a coherent motion at velocity  $V_{\text{bulk}}$  would lead to the dipole amplitude of  $V_{\text{bulk}}^2/c^2$ . When computed from the total of  $N_{\text{cluster}}$  positions the dipole of the noise term becomes  $\langle r^2(\nu) \rangle / N_{\text{cluster}}$ . The cosmological signal gives rise to two different dipole contributions: 1) the cosmological dipole has not been perfectly removed so the temperature anisotropies at the cluster locations sample the residual dipole  $\sigma_d$ ; and 2) even if all the cosmological dipole had been removed the intrinsic CMB temperature anisotropies could be seen as an extra dipole noise source. The latter contribute  $\sigma_{\text{CMB}}^2 / N_{\text{cluster}}$ , with  $\sigma_{\text{CMB}}$  being the variance of the cosmological temperature field on the smallest angular scales probed by the experiment. Thus for  $N_{\text{cluster}} \gg 1$  the dipole of (3) becomes:

$$C_{1,\nu} \simeq C_{1,kin} H^2(\nu) + C_{1,th} G^2(\nu) + [\sigma_{\text{CMB}}^2 / N_{\text{cluster}} + \sigma_d^2] H^2(\nu) + \langle r^2(\nu) \rangle / N_{\text{cluster}} \quad (1)$$

where it was assumed that for each individual X-ray cluster the thermal SZ term dominates.

### 3. Signal and noise terms.

We now estimate the amplitude of the signal,  $C_{1,kin}$ , and noise terms in eq. (1).

### 3.1. Kinematic component.

Assuming that cluster properties are independent of their velocities, this term is  $C_{1,kin} = T_0^2 \langle \tau_i \rangle^2 \frac{V_{bulk}^2}{c^2}$ .  $T_0$  is the CMB temperature, and  $i$  refers to the frequency band. The effective optical depth is affected by the beam dilution. To evaluate the expected mean optical depth accounting for the beam dilution effects we proceed as follows: for X-ray clusters the electron density profile can be approximated by the  $\beta$ -model. For isothermal and spherical X-ray gas distribution, the optical depth as a function of the angular distance from the cluster center would be  $\tau = \tau_0(1 + \theta^2 D^2 / r_{core}^2)^{-\frac{3\beta-1}{2}}$ . Here  $D$  is the distance to the cluster and  $r_{core}$  is its core radius. For each individual cluster observed in a CMB search, this expression needs to be convolved with the beam profile. The effective optical depth becomes  $\tau_i \equiv \tau_0 \Psi_i(D)$ , where  $\Psi_i$  accounts for the beam dilution effects. To evaluate  $\Psi_i(D)$  we compiled a list of 37 X-ray clusters with measured  $\beta, r_{core}$  and  $2.4 \text{ KeV} < T < 14.6 \text{ KeV}$  from Arnaud & Evrard (1999), Myers et al. (1997) and Neumann & Arnaud (1999). We then computed  $\Psi_i(D)$  for each individual cluster and the mean and the r.m.s. in  $\Psi_i(D)$  evaluated over the ensemble of clusters. Fig.1 plots the mean and the r.m.s. values of  $\Psi_i(D)$  vs  $D$  for the largest and smallest MAP beams. The figure shows that for the purposes of estimating the magnitude of the kinematic dipole component we can assume that a “universal” profile for the cluster optical depth exists to within an uncertainty of  $\sim 10\text{-}20\%$ .

The value of  $\langle \tau_0 \rangle$  can be estimated from the observed cluster properties and their X-ray luminosity function. Cooray (1999 - Table 1) compiled a list of 14 X-ray clusters with measured SZ thermal components,  $\Delta T_{SZ}$ , with the X-ray luminosity in the [2-10] KeV range,  $L_X(2\text{-}10 \text{ KeV})$ , between  $1.6 \times 10^{43}$  and  $3.6 \times 10^{45} h^{-2} \text{ erg/sec}$ . A linear regression fit to the data gives  $\tau_0 = (4.8 \pm 1.0) \times 10^{-3} [L_X(2\text{-}10 \text{ KeV}) / 10^{44} h^{-2} \text{ erg/sec}]^{\alpha_\tau}$  with  $\alpha_\tau = 0.41 \pm 0.12$ . Note that for isothermal X-ray clusters emitting due to thermal Bremsstrahlung,  $L_X \propto n_e^2 T_{virial}^{1/2}$ , and obeying the observed X-ray luminosity - temperature relation,  $L_X \propto T_{virial}^\gamma$  with  $\gamma \simeq 2.5$  (Mushotzky & Scharf 1997, Allen & Fabian 1998, Arnaud & Evrard 1998), one expects  $\tau \propto L_X^{0.4}$  (e.g. Haenelt & Tegmark 1996). These relations show little evolution out to  $z \sim 0.5$  (Mushotzky & Scharf 1997; Schindler 1999) and are valid for cluster catalogs of depth  $< 200 h^{-1} \text{ Mpc}$  needed for this project.

The mean optical depth can now be computed from measurements of the X-ray luminosity function (XLF). XLF has now been determined very accurately from the ROSAT BCS sample out to  $z \leq 0.3$  (Ebeling et al., 1997). The sample is 90% complete for fluxes  $\geq 4.45 \times 10^{-12}$  erg/cm<sup>2</sup>/sec in [0.1-2.4] KeV band. The XLF is of the Schechter type  $n(L_X)dL_X = n_*(L_X/L_*)^{\alpha_X} \exp(-L_X/L_*)dL_X$  with  $\alpha_X \simeq -1.8$  and bolometric  $L_* \simeq 9.3 \times 10^{44} h^{-2}$  erg/sec or  $L_*(2-10 \text{ KeV}) \simeq 3.2 \times 10^{44} h^{-2}$  erg/sec. For these XLF parameters and  $V_{\text{bulk}} = 600$  km/sec and a constant lower limit on the absolute X-ray luminosity  $L_0 \simeq 5 \times 10^{-3} L_*$ , corresponding to the [0.1-2.4]KeV flux  $4.5 \times 10^{-12}$  erg/cm<sup>2</sup>/sec at  $50 h^{-1}$  Mpc, we get  $\sqrt{C_{1,th}} \sim 9 \mu\text{K}$  dropping to  $\sim 6 \mu\text{K}$  for  $L_0 \simeq 2 \times 10^{-3} L_*$ .

### 3.2. Thermal component

The residual dipole from the SZ thermal component comes from the finite number of Poisson-distributed X-ray clusters and would integrate  $\propto 1/N_{\text{cluster}}$ . Since cluster properties are independent of position, the dipole contribution is  $C_{1,th} \simeq \langle (\Delta T_{SZ}) \rangle^2 \mathcal{D}_{\text{cluster}}^2$ . Here  $\langle (\Delta T_{SZ}) \rangle$  is the mean amplitude of the thermal SZ temperature fluctuation produced by the observed X-ray clusters and  $\mathcal{D}_{\text{cluster}} = \langle \cos \theta \rangle$ , with  $\theta$  being the cluster azimuthal angle, is the mean dipole of the cluster distribution out to the depth on which the bulk motions are probed. Assuming the scaling of  $\tau$  vs  $L_X$  above and integrating it over  $L_X \geq L_0 = \text{const}$  gives  $\langle (\Delta T_{SZ}) \rangle = 12 \mu\text{K}$  for  $L_0 = 0.002 L_*$  and  $\langle (\Delta T_{SZ}) \rangle = 20 \mu\text{K}$  for  $L_0 = 0.005 L_*$ . We used the Abell/ACO catalog (Abell 1958, Abell, Corwin & Olowin 1989) to verify that the angular distribution of clusters has  $\mathcal{D}_{\text{cluster}}^2 \propto N_{\text{cluster}}^{-1}$ . Statistically, one expects  $\mathcal{D}_{\text{cluster}}^2 N_{\text{cluster}} = 1/3$ . For the ACO catalogue out to  $200 h^{-1}$  Mpc we get  $\mathcal{D}_{\text{cluster}}^2 N_{\text{cluster}} \sim 0.2-0.3$ . The numbers are consistent with related dipole and monopole parameters of the gravitational field due to clusters ( $D_S, M_S = \sum r^{-2} \cos \theta, \sum r^{-2}$ ) from Fig.1 of Scaramella et al. (1991), when corrected for the fact that  $D_S, M_S$  are dominated by more nearby clusters. The different spectral dependence,  $G(\nu)$ , of thermal SZ can be used to reduce this term further. Thus the contribution of this term to the dipole noise term in eq. (1) would be  $\sqrt{C_{1,th}} < 10 N_{\text{cluster}}^{-1/2} \mu\text{K}$ . (The thermal component dipole can also be seen to be small from extrapolation to  $l=1$  from Figs. 1,2 in theoretical computation of the thermal SZ power spectrum by Atrio-Barandela & Mücke 1999, or Fig. 8 in Refreiger et al. 2000).

### 3.3. Dipole cosmological components.

There will be two independent contributions to the dipole noise from cosmological terms: from the residual dipole uncertainty and from the CMB fluctuations leaving a residual dipole when evaluated over a finite number of points on the sky ( $N_{\text{cluster}}$ ).

The first contribution will come from the cosmological dipole which can be eliminated from the CMB maps down to the 68% uncertainty of  $\sigma_d$  ( $=7\mu\text{K}$  for FIRAS). With  $N_{\text{cluster}}$  we will approach this systematic component as  $\sigma_d^2[1 + \text{O}(N_{\text{cluster}}^{-1})]$ . Because the correlation angle of the temperature anisotropies is larger than the pixel size, this component can be further decreased using a low-pass filter by performing the analysis on  $\delta(\vec{y}_{\text{cluster}}) - \delta(\vec{y}_{\text{ngb}})$ , where  $\vec{y}_{\text{ngb}}$  is the neighboring pixel that does not contain another cluster and is  $\Delta\theta_{\text{ngb}}$  away from the original pixel. The dipole noise will then be reduced to  $\sigma_d (\Delta\theta_{\text{ngb}}/180^\circ)$ , while the noise variance will increase by only  $1/N_{\text{ngb}}$ . The second contribution will come from the cosmological temperature anisotropy at each cluster location. The r.m.s. temperature anisotropy  $\sigma_{\text{CMB}}$  on the smallest scales probed by MAP is model dependent, but could be of the same order of magnitude as the pixel noise or even larger and it has the same frequency dependence as the kinematic SZ effect. Its contribution is  $\sigma_{\text{CMB}}^2/N_{\text{cluster}}$ , and can be reduced by the low-pass filtering discussed above. If necessary,  $\sigma_{\text{CMB}}$  can be reduced further with Wiener filtering (cf. Haenhelt & Tegmark 1996) designed to minimize the difference between the filtered signal,  $\tilde{\delta}_{\text{CMB}}$ , and the instrument noise,  $r$ . We computed the residual (Wiener-filtered) variance for two cold-dark-matter (CDM) models, the standard CDM with  $\Omega=1$ , and the cosmological constant dominated CDM with  $\Omega=0.3$  with  $\sigma_{\text{CMB}}=(57-93)\mu\text{K}$  in the MAP bands. After the filtering with the noise multipoles of MAP the numbers reduce to  $<\frac{1}{2}\langle r^2 \rangle^{1/2}$ ; this component adds in quadrature to the instrument noise.

### 3.4. Instrument noise component.

If the instrument noise in the given band is  $r(\nu)$ , its contribution to the dipole term in (1) is  $\langle r^2(\nu) \rangle / N_{\text{cluster}}^{-1}$ . The MAP mission (<http://map.gsfc.nasa.gov>) has 5 bands from 22 to 90 GHz and the r.m.s. noise at the end of two years should reach  $\langle r^2(\nu) \rangle^{1/2} = 35\mu\text{K}$  per  $0.3 \times 0.3$  deg pixel (the MAP beams range from 0.93 to 0.2 deg and its total lifetime would be at least 27 months). The

PLANCK satellite (<http://astro.estec.esa.nl/Planck>) has Low and High Frequency Instruments (LFI and HFI). The LFI has four bands from 30 to 100 GHz and the beams from 33 to 10 arcmin. Its noise at  $4\ \mu\text{K}$  at 30 GHz to  $12\ \mu\text{K}$  at 100 GHz is significantly lower than that of MAP. The six HFI bands cover 100 to 857 GHz and adding them would increase the signal-to-noise of the measurement of bulk flows with Planck. Because the instrument noise dipole would be added in quadrature to the cosmological component, this term is expected to be the dominant dipole noise term for MAP instruments.

#### 4. Results and strategies for measurement.

In order to apply this method we will take the available all-sky catalogs of imaged X-ray clusters and compute the dipole of the CMB temperature field at the cluster locations in the expectation that the noise terms will integrate down uncovering the bulk motion contribution to the dipole.

To measure the large-scale bulk flows by this method we need information on the location of  $\sim(100\text{--}300)$  X-ray clusters with reasonably measured  $\tau$ . A new all-sky catalog of imaged X-ray clusters should be available soon (Böhringer et al. 1999) from the ROSAT observations. The current catalog, known as BCS (Bright Cluster Sample), is  $\simeq 90\%$  complete in the Northern hemisphere and  $|b_{\text{Gal}}| \geq 20$  deg and contains 199 clusters with flux  $\geq 4.45 \times 10^{-12} \text{erg/cm}^2/\text{sec}$  (Ebeling et al. 1997). With the XLF parameters from Ebeling et al. (1997) a sphere of radius  $100h^{-1}\text{Mpc}$  would contain  $\sim 400$  X-ray clusters with  $L_{\text{X,bol}} \geq 10^{42} h^{-2} \text{erg/sec}$  (or  $10^{-3} L_*$ ),  $\sim 200$  clusters with  $L_X \geq 2.5 \times 10^{-3} L_*$  and  $\sim 100$  clusters with  $L_X \geq 5 \times 10^{-3} L_*$ . For flux-limited X-ray catalogs the numbers are similar: for flux limit of  $10^{-12} \text{erg/cm}^2/\text{sec}$  in the  $[0.1\text{--}2.4]$  KeV band of ROSAT, which is the flux limit of the NORA and REFLEX catalogs (Guzzo 2000), the number of clusters within  $100h^{-1}\text{Mpc}$  would be  $\simeq 200$  or  $\simeq 120$  for  $F \geq 2 \times 10^{-12} \text{erg/cm}^2/\text{sec}$ .

ROSAT has already completed a Southern hemisphere catalog of X-ray clusters, ROSAT-ESO Flux-Limited X-ray cluster survey or REFLEX, (Böhringer et al. 1999, Guzzo et al. 2000). The flux limit in the  $[0.1\text{--}2.4]$  KeV ROSAT band of the REFLEX survey is  $\sim 1.5 \times 10^{-12} \text{erg/cm}^2/\text{sec}$  corresponding to  $L_X(2\text{--}10\text{KeV}) \simeq 1.7 \times 10^{42} h^{-2} \text{erg/sec}$  at the distance of  $100h^{-1}\text{Mpc}$ . (Such clusters have  $\tau \sim 9 \times 10^{-4}$  and are quite numerous even at that depth avoiding the problem of significant



shot-noise from the rare and very high- $\tau$  clusters). The Northern hemisphere catalog of the ROSAT X-ray clusters (NORA) should be completed shortly (Guzzo 2000). Altogether this would result in approximately 1,500 X-ray clusters down to the limiting flux  $F \sim 1 \times 10^{-12}$  erg/cm<sup>2</sup>/sec in the [0.1–2.4] KeV band; out of these  $\sim 300$  would lie within  $\sim 100h^{-1}$  Mpc. In addition, there are already 50 X-ray clusters within  $\sim 100h^{-1}$  Mpc from ASCA searches which have both central temperature and electron density profile measured (Baumgartner et al 2000); this number is expected to more than double within the next year or two (Mushotzky, private communication). The ROSAT clusters can further be imaged very efficiently with XMM in order to obtain the necessary catalog of X-ray clusters by the time the MAP mission is completed.

Our ability to determine a bulk flow of amplitude  $V_{\text{bulk}}$  is limited by the instrumental noise term. The signal-to-noise ratio,  $\chi$ , in such a measurement out to the depth  $D$  would be given by:

$$\chi^2 = \sum_i \frac{\int_0^D C_{1,kin} dN_{\text{cluster}}}{r_i^2} = T_0^2 \frac{V_{\text{bulk}}^2}{c^2} N_{\text{cluster}} \left[ \frac{3}{D^3} \sum_i \frac{\int_0^D \langle \tau_0 \rangle^2 \Psi_i^2(D) D^2 dD}{r_i^2} \right] \quad (2)$$

The integral on the right-hand-side of eq. (2) accounts for the fact that the number of clusters contributing to the reduction in the dipole from the instrument noise in a thin shell  $[D; D + dD]$ , where the beam dilutes the central optical depth by  $\Psi_i(D)$ , is  $dN_{\text{cluster}} = 4\pi [\int_{L_0}^{\infty} n(L_X) dL_X] D^2 dD$ . For clusters selected from an absolute luminosity limited catalogs the term  $\langle \tau_0 \rangle^2$  in the integral on the RHS of eq.(2) would be independent of  $D$ ; for flux-limited catalog the dependence on  $D$  would come via  $L_0 \propto D^2$ . In computing  $\chi$  we assumed the mean shape of  $\Psi(D)$  plotted in Fig. 1.

If we want to determine just the amplitude of the bulk flow, we need the amplitude of the dipole SZ kinematic component. If we are to determine the direction of the flow, we need to measure all three dipole components:  $a_{1,1}, a_{1,0}, a_{1,-1}$ . Thus to determine the amplitude of the bulk velocity within a given  $D$  at the 95% c.l. we need  $\chi^2 = 3.84$ ; if we want to resolve all three components of the dipole at the 95% c.l., we need  $\chi^2 = 7.81$ . The error bar on the dipole components translates into an uncertainty on the measurement of the three components of the velocity flow, i.e., on the bulk flow direction. If all dipole components have been measured with the same precision, and the velocity of the flow is measured with an uncertainty  $\sigma_V$ , then the direction of the flow will be determined with an angular precision  $\delta\alpha = \sqrt{2}\sigma_V/V_{\text{bulk}}$ .

Fig. 2a shows the smallest  $V_{\text{bulk}}$  that can be determined at 95% c.l. with MAP and Planck/LFI data at  $D=50,100,150h^{-1}\text{Mpc}$  for a catalog with fixed lower bound of the bolometric X-ray luminosity,  $L_{0,\text{bol}}$ . The bulk velocity at  $150h^{-1}\text{Mpc}$  from Lauer & Postman (1994) is also shown for comparison. There is only a weak dependence in  $\chi^2$  on the (fixed) lower bound on the X-ray luminosity of the cluster catalog. Thus this method gives a very realistic way to measure the possible bulk flows on large scales or to significantly constrain their amplitude if the latter is small. Fig. 2b shows  $\chi^2$  vs the depth of the cluster catalog for the bulk flow of  $V_{\text{bulk}}=600\text{ km/sec}$  for MAP (lower set of lines) and Planck/LFI parameters (upper set of lines). Since  $\chi^2 \propto V_{\text{bulk}}^2$ , at the 95% c.l. the 2-year MAP data can probe in this way bulk flows with the amplitude as low as  $\simeq 250\text{ km/sec}$  on scale of  $\sim 100h^{-1}\text{Mpc}$ ; with Planck data such bulk flows can be probed to even much lower amplitudes and scales. Concerning the direction, MAP and Planck/LFI would determine á la Lauer-Potsman bulk flow direction with a 95% c.l. error of  $41^\circ$  and  $16^\circ$ , respectively.

Finally, because the upcoming X-ray catalogs, such as the NORA/REFLEX catalog, extend to significantly beyond  $100h^{-1}\text{Mpc}$  this method also would probe bulk flows on much larger scales. Fig.2c shows the amplitude of the bulk flow that can be determined at 95% c.l. vs the depth of the flux-limited X-ray cluster catalog. Bulk flows  $>100\text{km/sec}$  on scale  $\sim 300h^{-1}\text{Mpc}$  can be probed with this method with MAP data; with Planck/LFI this reduces to  $\sim 30\text{km/sec}$ . If MAP operates longer than 2 years, this number would decrease  $\propto t_{\text{operation}}^{-1/2}$ . If both LFI and HFI Planck channels are combined the bulk flows on large scales can be probed to even lower limits than with the Planck/LFI alone; e.g. on scale of  $\sim 100h^{-1}\text{Mpc}$  the amplitude of the bulk flows can be determined at 95% c.l. down to  $\sim 30\text{km/sec}$  and on scale of  $\sim 300h^{-1}\text{Mpc}$  to  $\sim 15\text{-}20\text{km/sec}$ .

AK acknowledges the hospitality and visiting support of the University of Salamanca. FAB acknowledges financial support of the Junta de Castilla y León (project SA 19/00B) and Ministerio de Educación y Cultura (project PB 96-1306). We thank Chuck Bennett, Gary Hinshaw, John Mather and Richard Mushotzky for fruitful discussions on CMB and X-ray parts of this work.

## REFERENCES

- Abell, G.O. 1958,Ap.J.Suppl.,**2**,211
- Abell, G.O., Corwin, H.G., & Olowin, R.P. 1989,Ap.J.Suppl.,70,1
- Allen, S.W. & Fabian, A.C. 1998, MNRAS, 297, L57
- Arnaud, M. & Evrard, A.E. 1999, MNRAS, 305, 631
- Atrio-Barandela, F. & Mücke, J. 1999,ApJ, 515, 465
- Baumgartner et al. 2000, AAS...
- Birkinshaw, M. 1999, Phys. Rep., 310, 97
- Böhringer, H. et al. 1999. Proceedings of the 14th IAP meeting: "Wide Field Surveys in Cosmology", Y. Mellier & S. Colombi (eds.). Preprint astro-ph/9809381.
- Cooray, A.R. 1999, MNRAS, 307, 841
- Ebeling, H. et al., 1997, ApJ, 479, L101
- Fixsen, D. J. et al. 1996, ApJ, 473, 576
- Guzzo, L. 2000,astro-ph/9911115
- Guzzo, L. et al. 2000,astro-ph/9903396
- Haehnelt, M. G. & Tegmark, M. 1996, MNRAS, 279, 545
- Lauer T.R. & Postman, M. 1994, ApJ, 425, 418
- Mushotzky, R.F. & Scharf, C.A. 1997, ApJ, 482, L13
- Myers, S.T. et al. 1997, ApJ, 485, 1
- Neuman, D.M. & Arnaud, M. 1999, A&A, 348, 711

Phillips, P.R. 1995, ApJ, 455, 419

Refregier, A. et al. 2000, preprint, astro-ph/9912180

Scaramella, R., Vettolani, G. & Zamorani, G. 1991, ApJ, 376, L1

Schindler, S. 1999, A&A, 349, 435

Willick, J. 2000, in proceedings “XXXVth Rencontres de Moriond: Energy Densities in the Universe”, astro-ph/0003232

Zeldovich, Ya. B., Sunyaev, R. 1969, Ap&SS, 4, 301

## FIGURE CAPTIONS

**Fig. 1:** The dilution factor  $\Psi(D)$  vs the depth  $D$  for two MAP bands. Solid lines are for Gaussian beam corresponding to Band 1 (22 GHz, FWHM = 0.93 deg). Dashed lines are for Band 5 (90 GHz, FWHM = 0.21 deg). Thick lines correspond to the cluster profile averaged over 37 X-ray clusters as described in the main text. Thin lines correspond to the r.m.s. value of  $\Psi(D)$  over the same sample.

**Fig. 2:** (a) The amplitude of  $V_{\text{bulk}}$  that can be determined at 95% c.l. ( $\chi^2 = 3.84$ ) is plotted vs the lower limit on the bolometric X-ray luminosity,  $L_{0,\text{bol}}$ . Thin lines correspond to MAP and thick lines to Planck/LFI data parameters. Solid lines correspond to X-ray clusters out to  $D = 50, 100, 150h^{-1}\text{Mpc}$  from top to bottom respectively. From top to bottom, dashed lines show the value of  $V_{\text{bulk}}$  when the three components of the dipole can be determined at the 95% c.l. at  $D = 50, 100, 150h^{-1}\text{Mpc}$ , respectively. Open square with error bar shows the amplitude of the bulk flow at  $150h^{-1}\text{Mpc}$  from Lauer & Postman (1994). (b) Solid lines plot  $\chi^2$  from eq. (2) vs the depth of the X-ray cluster catalog,  $D$ , with a cutoff on the X-ray luminosity of  $L_0/L_* = (1, 2, 5) \times 10^{-3}$  from top to bottom respectively. Dotted lines correspond to flux-limited X-ray cluster catalog with the  $[0.1-2.4] \text{ KeV flux} \geq (1, 2) \times 10^{-12}\text{erg/cm}^2/\text{sec}$ . Lower set of lines is for MAP data and the upper set of lines is for the Planck/LFI instrument parameters. In the latter case over the range of the plot the two lines for the  $[0.1-2.4] \text{ KeV flux} \geq (1, 2) \times 10^{-12}\text{erg/cm}^2/\text{sec}$  coincide with each other and with the  $L_X/L_* \geq 10^{-3}$  case. Thick solid horizontal line corresponds to  $\chi^2 = 3.84$ , when the amplitude of the bulk flow can be determined at 95% confidence level; thick dashed horizontal line corresponds to  $\chi^2 = 7.81$ , when the three components of the dipole can be determined at 95% confidence level. (c) The amplitude of the bulk flow that can be determined at 95.4% c.l. is plotted vs the depth of the flux-limited X-ray cluster catalog. Solid lines correspond to the MAP data, thin dotted lines to Planck/LFI and thick solid lines to Planck/LFI and Planck/HFI together. Two sets of lines correspond to X-ray flux  $\geq (1, 2) \times 10^{-12}\text{erg/cm}^2/\text{sec}$  from top to bottom respectively.

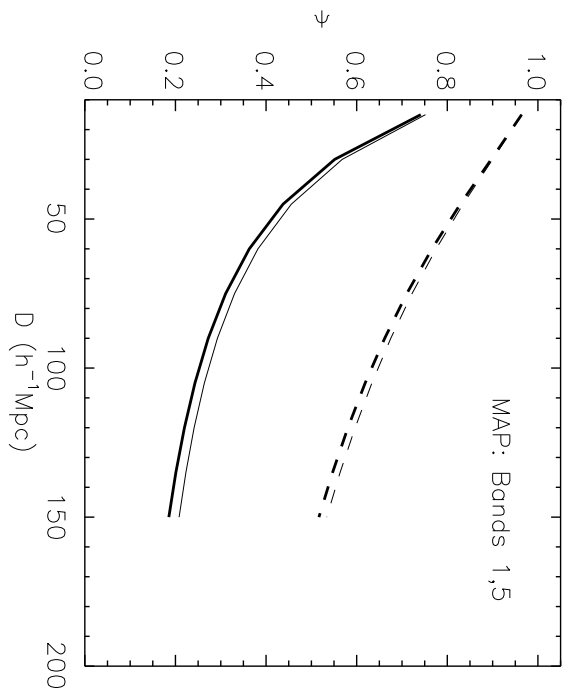


Fig. 1.—

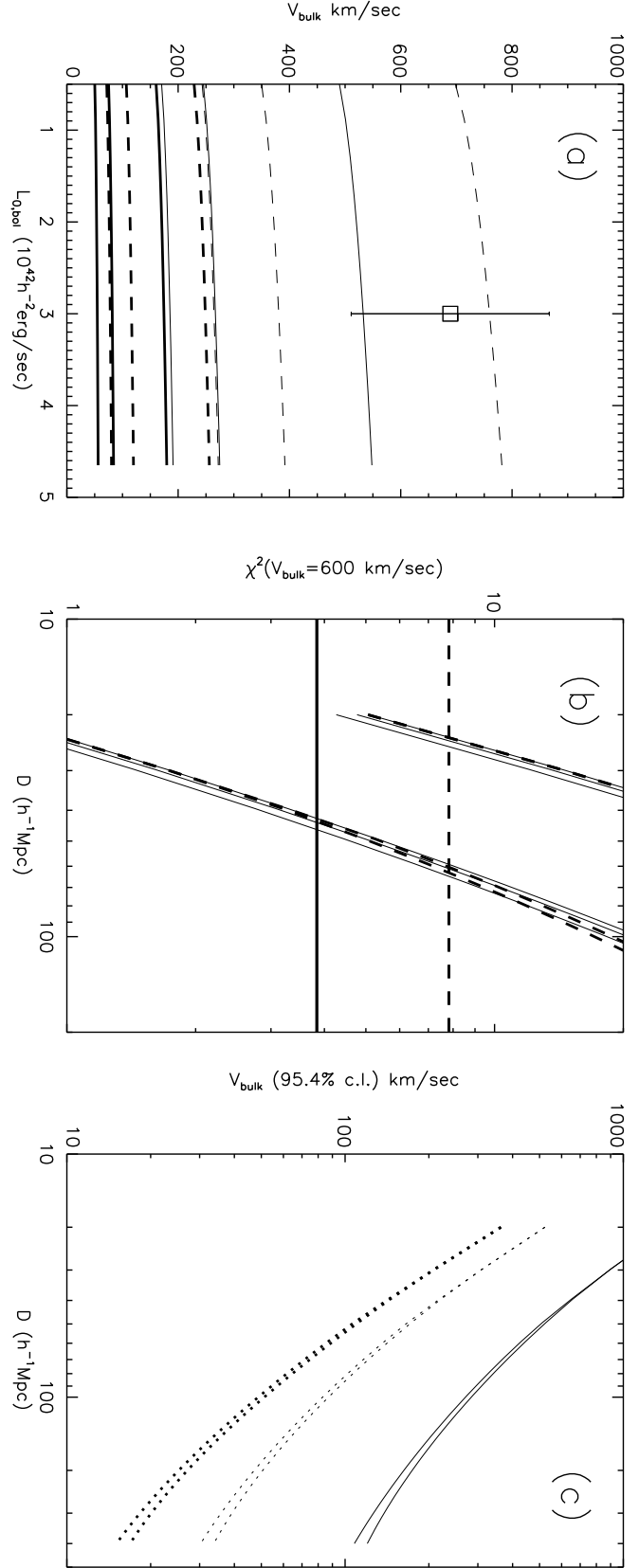


Fig. 2.—